Quantile ARDL Estimation of the Relationship between the Confirmed COVID-19 Cases and Deaths in the U.S.

XIN JING
School of Economics, Yonsei University, Seodaemun-gu, Seoul 03722, Korea
Email: superheunheun@gmail.com

JIN SEO CHO
School of Economics, Yonsei University, Seodaemun-gu, Seoul 03722, Korea
Email: jinseocho@yonsei.ac.kr

This version: June 18, 2025

Abstract

This study exploits the quantile ARDL model to investigate the dynamic relationship between the confirmed COVID-19 cases and deaths in the U.S. following vaccination, with a focus on examining heterogeneity across different percentiles. The findings indicate that the confirmed case fatality rate decreased after vaccination, and the relationship between confirmed cases and deaths varies across different percentiles.

Key Words: Quantile ARDL; Cointegration; COVID-19; Vaccination; Heterogeneity.

JEL Classifications: C12, C22, I18.

Acknowledgements: Cho acknowledges financial support from the Ministry of Education of the Republic of Korea and the National Research Foundation of Korea (NRF-2020S1A5A2A01040235).

1 Introduction

Since the onset of COVID-19, countries around the world have implemented stringent control measures to curb the spread of the virus, and these measures have also incurred significant economic costs, resulting in unprecedented economic losses (Forsythe, Cohen, Neumann, Bertozzi, and Kinghorn, 2020; Deb, Furceri, Ostry, and Tawk, 2022b).

Meanwhile, vaccination campaigns have had a substantial positive impact on economic recovery from a health economics perspective (Utami, Rendrayani, Khoiry, Noviyanti, Suwantika, Postma, and Zakiyah, 2023; Hansen and Mano, 2023), and have also been highly effective in reducing confirmed cases and deaths.

However, hesitancy and refusal to be vaccinated continue to undermine the effectiveness of these interventions. Vaccine hesitancy and refusal not only have the potential to counteract all efforts to control the pandemic, but also have profound impacts on the global economy (e.g., Rawlings, Looi, and Robson, 2022). According to Padula, Malaviya, Reid, Cohen, Chingcuanco, Ballreich, Tierce, and Alexander (2021), annual productivity losses caused by unvaccinated workers are predicted to amount to USD 15 billion, despite vaccinations having already reduced COVID-related costs by approximately 80%. In addition, hesitancy and refusal to receive vaccines exhibit significant heterogeneity. Goel, Jones, and Saunoris (2023) demonstrate that US states with higher wealth, a larger elderly population, and more physicians tend to have lower levels of vaccine hesitancy. In addition, hesitancy to get vaccines is correlated with educational level, age, vaccine characteristics, vaccination methods, and media coverage (e.g., Kountouris and Remoundou, 2024; Tan, Straughan, and Cheong, 2022; McPhedran and Toombs, 2021). All of this implies that different groups have been impacted by both the virus and the vaccination campaign heterogeneously.

In the current study, we focus on the fatality rate of COVID-19 that associates confirmed cases with deaths and empirically examine how the rate is formed heterogeneously while taking into account the vaccination effect. For this, we characterize the underlying heterogeneity by the risk of confirmed cases exposed to death and employ the Quantile Autoregressive Distributed Lag (QARDL) estimation proposed by Cho, Kim, and Shin (2015), which facilitates revealing the heterogeneity of the death rate.

The analysis of the fatality rate taking into account heterogeneity is unique in the literature. Ullah, Wang, and Yao (2022) note significant differences exist in the number of confirmed cases and deaths across the US states, providing valuable insights into asymmetric economic activities. Mehta, Gupta, and Maitra (2023) and Chang, Gohar, Derindag, and Uche (2023) also apply the Autoregressive Distributed-Lag (ARDL) model to analyze the impact of COVID-19 on real estate, food industries, and healthcare industries. Nevertheless, no prior literature takes into account heterogeneity while analyzing the fatality rate to our knowl-

edge.

QARDL is useful in detecting heterogeneity in the fatality rate and examining the vaccination effect. It is widely acknowledged that the currently published COVID-19 data often contain noise, outliers, biases, skewness, and truncation issues (e.g., Jing and Cho, 2025). Meanwhile, Jiang, Zhao, and Shao (2022) demonstrate that quantile regression is robust in handling outliers and capturing heterogeneity by focusing on the short-term forecasts of the confirmed cases. Given that QARDL applies quantile regression to nonstationary series, we exploit its useful features to estimate the fatality rate defined as the long-run relationship between the confirmed cases and deaths.

The remainder of this paper is organized as follows. Section 2 provides a comprehensive review of the literature that forms the basis and motivation for this study. Section 3 details the QARDL estimation methodology, highlighting its theoretical framework and advantages over conventional approaches. Section 4 presents the empirical analysis, in which we investigate the dynamic relationship between confirmed COVID-19 cases and deaths across different percentiles. Finally, Section 5 summarizes the key findings, discusses their policy implications, and outlines directions for future research.

2 Literature Review

Amid the global health crisis, an increasing number of studies examine infection and death counts during the COVID-19 pandemic. These studies help to understand viral transmission and fatality mechanisms and offer valuable guidance for public health policymaking. As vaccination coverage continues to expand, the nature of this dynamic relationship evolves, and it warrants further investigation into the potential heterogeneity under widespread vaccination. Drawing on the existing literature, we review the determinants of COVID-19 fatality, the role of vaccination, recent findings on the dynamic case-fatality relationship, and the latest methodological advances for empirical analysis.

Existing studies show that multiple factors influence COVID-19 fatality. First, demographic characteristics, such as age and gender, play a decisive role in fatality differences (e.g., Verity, Okell, Dorigatti, Winskill, Whittaker, Imai, Cuomo-Dannenburg, Thompson, Walker, Fu et al., 2020; Torres, García, Meslé, Barbieri, Bonnet, Camarda, Cambois, Caporali, Couppié, Poniakina et al., 2023; OâĂŹDriscoll, Ribeiro Dos Santos, Wang, Cummings, Azman, Paireau, Fontanet, Cauchemez, and Salje, 2021). Second, chronic underlying conditions, such as hypertension, diabetes, and cardiovascular diseases, significantly increase the risk of death (e.g., Lee and Hwang, 2025). In addition, the adequacy of medical resources, such as the number of general practitioners and hospital beds per capita, as well as government interventions, including

lockdown policies, social distancing, and travel restrictions, also have important effects on fatality (e.g., Di Porto, Naticchioni, and Scrutinio, 2022; Fang, Wang, and Yang, 2020).

Widespread vaccination serves as a crucial measure in controlling the pandemic. Multiple empirical studies demonstrate that vaccines significantly reduce infection and severe illness rates, thereby indirectly lowering fatality (e.g., Kim and Lee, 2022). However, vaccine effectiveness exhibits spatial and population heterogeneity, as elderly individuals, immunocompromised patients, and viral variants may affect vaccine efficacy (e.g., Tiu, Susswein, Merritt, and Bansal, 2022; Mori, Yokoyama, Shichida, Sasuga, Maekawa, and Moriyama, 2023). Some studies also suggest that the protective efficacy of vaccines may gradually decline over time following vaccination (e.g., Suah, Husin, Tok, Tng, Thevananthan, Low, Appannan, Zin, Zin, Yahaya et al., 2022).

Existing studies suggest that there is a dynamic lag relationship between confirmed cases and deaths (e.g., Jin, 2021). Some studies employ time series models to forecast and analyze the number of confirmed COVID-19 cases and deaths (e.g., Liu, Moon, and Schorfheide, 2021; Gupta and Pal, 2020; Sujath, Chatterjee, and Hassanien, 2020). The traditional ARDL model, due to its favorable properties in small samples, has been widely applied in COVID-19 pandemic analysis (e.g., Chang et al., 2023; Jeris and Nath, 2020). However, the ARDL model assumes homogeneity in the relationships between variables across all levels, which fails to capture the influence of heterogeneity on fatality rate under different severity conditions.

In recent years, quantile regression has been widely applied in health research to reveal heterogeneous effects across different points of distribution (e.g., Okada, 2018; Chen, Ma, Sundell, Alaka, Schuh, Raskin, and Dean, 2016; Silva, Simões, and Andrade, 2018). In the context of COVID-19 research, quantile regression methods can identify the variational mechanisms between confirmed cases and deaths under different levels of disease severity, particularly capturing the dynamic features at extreme values, such as periods of high fatality risk (e.g., Jiang et al., 2022; Ribeiro, Cordeiro, Pena-Ramirez, and Guerra, 2021).

The QARDL model combines the dynamic properties of ARDL with quantile regression to identify heterogeneity, allowing for the estimation of both short- and long-run dynamics across different percentiles. In the fields of macroeconomics and finance, QARDL has been popular in effectively capturing nonlinearity and distributional heterogeneity (e.g., Cho et al., 2015; Hammoudeh, Mensi, and Cho, 2022). However, its application in health economics remains relatively new, particularly in the analysis of COVID-19 data.

Overall, although the existing literature has extensively examined the determinants of COVID-19 fatality and the effectiveness of vaccination, systematic empirical evidence is lacking on whether quantile-dependent dynamic differences exist between confirmed cases and deaths in the post-vaccination period. This study employs QARDL methodology to systematically analyze the dynamic relationship between confirmed cases

and deaths across different percentiles in the context of vaccination in the U.S., providing more nuanced evidence for understanding the evolution of the pandemic and offering new empirical insights for public health policymaking.

3 QARDL Estimation and Inference

Cho et al. (2015) extend the ARDL approach by applying the quantile regression and jointly analyze the short- and long-run relationships across a range of percentiles, which is known as the QARDL methodology. In this section, we apply the QARDL methodology to COVID-19 data.

The QARDL methodology assumes different cointegrating coefficients depending on the percentile. Specifically, it assumes the following relationship:

$$Y_t = \alpha_*(\tau) + \sum_{j=1}^{p} \phi_{j*}(\tau) Y_{t-j} + \sum_{j=0}^{q} \boldsymbol{\theta}_{j*}(\tau)' \mathbf{X}_{t-j} + U_t(\tau).$$

This specification is commonly referred to as QARDL(p, q) process. Here, $\Delta \mathbf{X}_t$ is assumed to be a k-dimensional stationary ergodic process ($k \in \mathbb{N}$); the error term $U_t(\tau)$ is defined as $Y_t - Q_\tau(Y_t|\mathcal{F}_{t-1})$, where $Q_\tau(Y_t|\mathcal{F}_{t-1})$ is the conditional quantile function on $\mathcal{F}_{t-1}$; $\mathcal{F}_{t-1}$ is the smallest σ-field generated by $\{\mathbf{X}_t', Y_{t-1}, \mathbf{X}_{t-1}', \ldots\}$; and p and q are the QARDL lag orders such that $U_t(\tau)$ is identically and independently distributed.

Based on the existing empirical and theoretical analysis, we suppose the current death D_t and the confirmed case C_t are cointegrated. It is widely accepted that there exists a long-run relationship between confirmed cases and deaths, represented as

$$D_t = \beta_* C_t + \varepsilon_t,$$

where β_* denotes the long-run fatality rate (e.g., Brodeur, Gray, Islam, and Bhuiyan, 2021). Here, ε_t represents the cointegration error. If ε_t is stationary, the QARDL process is rewritten as follows:

$$\triangle D_t = \alpha_* + \zeta_* D_{t-1} + \gamma_* C_{t-1} + \sum_{j=1}^{p-1} \lambda_{j*} \triangle D_{t-j} + \sum_{j=0}^{q-1} \delta_{j*} \triangle C_{t-j} + U_t$$

such that U_t is identically and independently distributed, which is ensured by letting the lag orders p and q be sufficiently large. By substituting the cointegrating relationship $D_{t-1} = \beta_* C_{t-1} + \varepsilon_{t-1}$, we obtain the

following ARDL(p, q) process:

$$\triangle D_t = \alpha_* + \zeta_*(D_{t-1} - \beta_* C_{t-1}) + \sum_{j=1}^{p-1} \lambda_{j*} \triangle D_{t-j} + \sum_{j=0}^{q-1} \delta_{j*} \triangle C_{t-j} + U_t \tag{1}$$

where $\beta_* := -\frac{\gamma_*}{\zeta_*}$.

We are interested in estimating the parameters in (1). Each parameter has the following interpretations. First, the Error Correction Model (ECM) parameter ζ_* measures the smoothing fatality that reflects the adjustment speed of the death toward the long-run equilibrium with the confirmed case. Second, the long-run cointegration coefficient β_* measures the fatality rate. Third, the momentum effect of death growth $\lambda_* := \sum_{j=1}^{p-1} \lambda_{j*}$ measures the cumulative impact of the lagged changes in D_t on the current death, viz., $\sum_{j=1}^{p-1} \partial \triangle D_t / \partial \triangle D_{t-j}$. Finally, the impulse response coefficient of the death change to the newly confirmed cases, viz., $\delta_* := \sum_{j=0}^{q-1} \delta_{j*}$, assesses the impact of the most recent changes in the confirmed case on the current death change. It is worth emphasizing that δ_* measures the short-run impact of the change in newly confirmed cases on the change in deaths. It accounts for the effect of the multiple lags, whereas β_* describes the relationship between the number of newly confirmed cases and deaths, reflecting the long-run fatality rate of the pandemic. In short, δ_* focuses on the short-run dynamic adjustment, while β_* represents the long-run fatality rate of the pandemic.

Based on their definitions, the signs of some parameters are predetermined. First, $-1 < \zeta_* < 0$ is implied by the long-run relationship between C_t and D_t. A significant and negative coefficient implies a strong corrective force toward the long-run equilibrium. Second, $0 < \beta_* < 1$ is implied from the long-run relationship. The long-run relationship between C_t and D_t can be neither negative nor greater than unity by definition.

We extend the ARDL expression to QARDL specification and allow for heterogeneous relationships between the confirmed cases and deaths. For each percentile $\tau \in (0, 1)$, we let the following be the QARDL(p, q) model:

$$\triangle D_t = \alpha_*(\tau) + \zeta_*(\tau)(D_{t-1} - \beta_*(\tau) C_{t-1}) + \sum_{j=1}^{p-1} \lambda_{j*}(\tau) \triangle D_{t-j} + \sum_{j=0}^{q-1} \delta_{j*}(\tau) \triangle C_{t-j} + U_t(\tau). \tag{2}$$

This specification allows the coefficients in (1) to be different from those of different percentiles so that heterogeneous cointegrating relationships exist between D_t and C_t.

The QARDL model captures the heterogeneity by the risk level of death. The confirmed patients with a high level of percentile are likely to face death sooner than those with a low level of percentile, from which

we use the risk of death as the heterogeneity index. As Ullah et al. (2022) point out, there are significant differences in the projections of the COVID-19 confirmed cases and deaths across the US states. (see also Deb, Furceri, Jimenez, Kothari, Ostry, and Tawk, 2022a; Hansen and Mano, 2023). This suggests potential systematic variations in the fatality rate, leading to heterogeneous relationships for different groups. The QARDL model in (2) assumes the risk of death as a summary index representing heterogeneous groups.

We apply the Wald test principle to the estimated coefficients and identify the heterogeneous relationship. Specifically, we test for different relationships between confirmed cases and deaths across percentiles. The following four null hypotheses are considered:

$$H_0^{\zeta} : \zeta_*(0.25) = \zeta_*(0.5) = \zeta_*(0.75), \qquad H_0^{\beta} : \beta_*(0.25) = \beta_*(0.5) = \beta_*(0.75),$$

$$H_0^{\lambda} : \lambda_*(0.25) = \lambda_*(0.5) = \lambda_*(0.75), \qquad H_0^{\delta} : \delta_*(0.25) = \delta_*(0.5) = \delta_*(0.75).$$

The heterogeneous relationship provides valuable policy implications. For example, strategically developed control measures can be implemented to curb the spread of the virus efficiently to the extent of heterogeneity. As another example, the vaccination campaign can result in different consequences depending on the heterogeneity.

4 Empirical Analysis

In this section, we conduct empirical analysis by applying the QARDL methodology to empirical data in the U.S.

First, we describe the data used in this study. The US COVID-19 confirmed case and death data are obtained from the World Health Organization's Coronavirus Dashboard.[1] Given the crucial role of vaccination in the progress of the pandemic, we explicitly incorporate the timing of vaccine administration into our sample selection. The first COVID-19 vaccine dose was administered on December 8, 2020 outside of clinical trials. As of December 8, 2021, approximately 55.9% of the global population received at least one dose; 45.5% completed two doses; and 4.3% received booster shots.

Based on these key vaccination milestones, we let the sample period from December 8, 2020 to December 7, 2021. This sample period enables us to analyze the dynamic relationship between confirmed cases and deaths in the context of large-scale vaccination efforts. All data are collected daily to capture the fluctuations and potential dynamic features between the two variables.

[1]The data are available at the following URL: https://ourworldindata.org/covid-vaccinations.

4.1 Full Sample Analysis

We report the QARDL estimation results based on the full sample. According to the Bayesian information criterion (BIC), the lag orders are set to $p = 7$ and $q = 2$. As shown in Table 1, the estimated coefficients are statistically significant across all percentiles, indicating that the model specification is robust and heterogeneous dynamic relationships exist across different percentile levels.

To better illustrate the quantile-dependent effects, we plot the estimation results in Figure 1. The figure presents the estimated trajectories of the four key parameters: $\zeta_*(\tau)$, $\beta_*(\tau)$, $\lambda_*(\tau)$, and $\delta_*(\tau)$ across the percentiles ranging from 0.1 to 0.9. We also provide the 90% confidence bands of the estimated parameters, by which we can assess the precision and statistical significance of the estimates at each percentile.

The quantile-specific coefficient estimates reveal clear evidence of location asymmetry, indicating that the dynamic relationship between confirmed cases and deaths systematically varies across different levels of pandemic severity. In particular, the heterogeneous effects captured by the QARDL model highlight that the distributional effect produces different estimates for different percentiles, which is often overlooked in the conventional mean-based model estimation.

We summarize the estimation results as follows. First, the estimated error correction model (ECM) parameter $|\zeta_*(\tau)|$ indicates a clear downward trend in adjustment speed for the increase in the percentile level. Specifically, at lower percentiles (e.g., $\tau = 0.1$), the adjustment speed reaches as high as 33.2%, implying that the system corrects deviations from the long-run equilibrium at a relatively faster pace under lower fatality risk conditions. This suggests that short-term fluctuations in the relationship between confirmed cases and deaths are more easily absorbed and stabilized under mild pandemic conditions. In contrast, at higher percentiles (e.g., $\tau = 0.9$), the estimated adjustment speed drops sharply to 7.6%, indicating that the convergence to the long-run equilibrium is substantially slower under high fatality risk conditions. This slower adjustment process reflects that all the factors such as overloaded healthcare system, shortage of medical resources, delays in reporting, and increasing uncertainty regarding treatment effectiveness may contribute to the prolonged deviation from equilibrium during the severe phase of the pandemic. From this finding, we can conclude that the heterogeneity in adjustment speeds across percentiles contributes to the joint distribution between confirmed cases and deaths.

Second, the estimation results of the fatality rate $\beta_*(\tau)$ reveal a clear upward trend for the increase in the percentile level, indicating another significant heterogeneity across different percentiles. At lower percentile levels (e.g., $\tau = 0.1$), the estimated fatality rate is relatively low, with $\beta(\tau) = 0.01$, suggesting that the proportion of deaths relative to confirmed cases remains small under mild pandemic conditions. This

reflects that most infected individuals experience mild symptoms or receive timely and adequate medical treatment under lower infection risks. In contrast, at higher percentile levels (e.g., $\tau = 0.9$), the fatality rate rises sharply to 0.04, indicating that under more severe pandemic conditions, the death count increases substantially relative to confirmed cases. This sharp rise can be associated with overwhelmed healthcare systems, the shortage of intensive care resources, or a higher proportion of vulnerable groups such as the elderly and individuals with pre-existing medical conditions. These findings further support the view of Ullah et al. (2022) that significant variations in COVID-19 fatality rates exist in the U.S., and our model effectively captures this feature through the heterogeneous risk of death across different percentiles.

Third, the estimation results of the momentum parameter $\lambda_*(\tau)$ show a decreasing trend for the increase in the percentile level, declining from -2.27 at $\tau = 0.1$ to -3.60 at $\tau = 0.9$. This pattern indicates that the momentum effect gradually strengthens at higher percentile levels. Specifically, the increasingly negative value of $\lambda_*(\tau)$ suggests that past deaths exert a stronger suppressive effect on current deaths as the severity condition of the pandemic intensifies. At lower percentile levels, where the fatality risk is relatively mild, a weaker moment parameter is estimated. The weaker momentum effect implies that current deaths are less influenced by their past values. In contrast, the momentum effect becomes more pronounced at higher percentile levels, indicating that past deaths have a stronger dampening impact on current deaths.

Fourth, the estimated response coefficient $\delta_*(\tau)$ fluctuates between 0.008 and 0.01 across all the percentiles, indicating a positive impact of a short-run fluctuation in confirmed cases on the change in deaths. This result highlights that even low levels of variation in confirmed cases affect the death count in the short term.

Finally, we conduct parameter heterogeneity tests across percentiles. In the bottom panel of Table 1, we report the Wald test statistics for the null hypotheses described in Section 3. The test results strongly reject the null hypotheses for $\zeta_*(\tau)$, $\beta_*(\tau)$, and $\lambda_*(\tau)$, indicating that the parameters exhibit significant heterogeneity across different percentiles. This suggests that the error correction speed, fatality rate, and momentum effect all vary substantially with the severity condition of the pandemic. This further highlights the importance of incorporating quantile-dependent dynamics when analyzing the relationship between confirmed cases and deaths. In contrast, the test for $\delta_*(\tau)$ fails to reject the null hypothesis, suggesting that the short-run dynamics captured by $\delta_*(\tau)$ does not show a significant variation across different risk levels.

4.2 Sub-Sample Analysis

In this section, we examine the impact of the vaccination campaign on the parameters across different percentiles over different sample periods.

To this end, we first plot the estimates of the four parameters. Figure 2 shows the estimates obtained using observations in numerous samples, along with their 90% confidence bands. A robust rolling estimation technique with a window length of 266 days is employed to ensure sufficient observations. Specifically, the rolling window approach shifts the sample window forward by one day at a time until the end of the sample period is reached. This approach enables us to dynamically track the evolution of the parameter estimates in response to changes in the pandemic and vaccination. As shown in Figure 2, the rolling quantile regression estimates display pronounced time-varying patterns across different percentile levels. This indicates that the relationship between confirmed cases and deaths is not only heterogeneous across percentiles but also dynamically evolves.

We examine the estimated parameters specifically. First, the estimated degree of smoothing fatality $|\zeta_*(\tau)|$ decreases as the percentile increases throughout the entire period. In the early period, location asymmetry is relatively strong with the average adjustment speed being approximately 22.0%, 14.0%, and 12.0% for $\tau = 0.25$, $\tau = 0.5$, and $\tau = 0.75$, respectively. In the middle period, location asymmetry peaks at 30.0%, 20.0%, and 10.0%, respectively. However, the location asymmetry weakens in the later period. All the estimated values are about 20% for all the percentiles. It is worth noting that the U.S. began its vaccination campaign in December 2020 and accelerated its schedule in the spring of 2021. During the first few months of the year, a broad vaccination infrastructure was established, and this led to significant changes in the parameter estimates for the period from 21/02/12 to 21/11/04.

Second, the rolling quantile regression estimates of $\beta_*(\tau)$ show a clear downward trend, indicating that the fatality rate has significantly decreased after the vaccination campaign began. In addition, $\beta_*(\tau)$ exhibits significant location asymmetry throughout the entire period such that the estimated $\beta_*(\tau)$ increases as τ increases. In the early period, the fatality rate is approximately estimated as 1.20%, 1.70%, and 2.20% for $\tau = 0.25$, $\tau = 0.5$, and $\tau = 0.75$, respectively. However, these estimated rates drop to 1.10%, 1.40%, and 1.80% over time, respectively. From this, we can conclude that the fatality rate has declined with a more pronounced decline at the higher percentiles. That is, the vaccination has impacted the group with a higher risk of death.

Third, the momentum effect of the death change exhibits a location asymmetry in the later period, with $\lambda_*(\tau)$ being -3.0, -3.5, and -4.0 at $\tau = 0.25$, $\tau = 0.5$, and $\tau = 0.75$, respectively. In contrast, the rolling quantile regression estimates of $\zeta_*(\tau)$ remain stable at around 0.005 throughout the entire sample period.

Finally, we present the p-values of the Wald tests based on the rolling estimates in Figure 3. The results show that the null hypotheses of parameter constancy for $\zeta(\tau)$ and $\beta(\tau)$ are strongly rejected throughout the entire sample period, indicating that both the error correction speed and fatality rate exhibit persistent

heterogeneity over time and across different percentiles. This suggests that even under continuous vaccination progress, both the adjustment process toward long-run equilibrium and the fatality dynamics remain highly sensitive to evolving pandemic conditions. However, the location asymmetry of $\lambda(\tau)$ is statistically significant only in the later sample period. This finding reflects that as the pandemic evolves, the dynamic feedback between past and current deaths becomes increasingly complex and asymmetric. In contrast, the test results for $\zeta_*(\tau)$ indicate that its location asymmetry is not statistically significant throughout the entire period, suggesting a relatively stable behavior over time.

Taken together, these findings confirm the existence of significant asymmetries in the dynamic relationship between confirmed cases and deaths. More importantly, the continued presence of heterogeneity even after the large-scale vaccination implies that it has not eliminated the underlying distributional differences in how the pandemic affects various segments of the population. This further highlights the need for flexible and risk-sensitive public health policies that fully account for such heterogeneous effects in the post-vaccination phase.

5 Conclusion

This study exploits the QARDL methodology and empirically examines the heterogeneous dynamic relationship between confirmed COVID-19 cases and deaths. Further, we investigate the role of vaccination campaigns in shaping this relationship. The heterogeneity across different groups is assessed based on the varying risks of death faced by confirmed patients. The empirical results reveal significant differences in the dynamic linkage between infections and fatalities across different levels of death risk. In particular, the vaccination campaigns have played a crucial role in reducing the COVID-19 fatality rate, especially for high-risk groups, although heterogeneity in fatality rates has persisted.

These findings obtained by introducing a quantile-based framework contribute to the existing literature that often overlooks heterogeneity in conventional empirical analysis. The study also offers important implications for public health policymakers, highlighting the need for targeted vaccination strategies and resource allocation to protect vulnerable populations more effectively. As the pandemic continues to evolve with the emergence of new variants and vaccine-induced immunity potentially declines, further research is warranted to explore the long-term dynamics and to refine policy interventions accordingly.

Although this study provides important insights into the quantile-dependent dynamic relationship between confirmed COVID-19 cases and deaths, several directions remain for future research. First, as new variants continue to emerge, future studies need to incorporate variant-specific data to examine whether the

heterogeneous effects identified in this study persist or change across different virus strains. Second, more detailed individual-level data can be employed to capture heterogeneity more efficiently across demographic groups, such as age, comorbidities, and vaccination status. Finally, the QARDL framework can be extended to multi-country panel data to conduct cross-country comparisons and assess how different healthcare systems, public health interventions, and vaccination strategies influence the short- and long-run relationships between confirmed cases and deaths.

References

BRODEUR, A., D. GRAY, A. ISLAM, AND S. BHUIYAN (2021): "A literature review of the economics of COVID-19," *Journal of Economic Surveys*, 35, 1007–1044.

CHANG, B. H., R. GOHAR, O. F. DERINDAG, AND E. UCHE (2023): "COVID-19, lockdown measures and their impact on food and healthcare prices: Empirical evidence using a dynamic ARDL model," *Journal of Economic Studies*, 50, 1008–1026.

CHEN, Y.-F., X. MA, K. SUNDELL, K. ALAKA, K. SCHUH, J. RASKIN, AND R. A. DEAN (2016): "Quantile regression to characterize solanezumab effects in Alzheimer's disease trials," *Alzheimer's & Dementia: Translational Research & Clinical Interventions*, 2, 192–198.

CHO, J. S., T.-H. KIM, AND Y. SHIN (2015): "Quantile cointegration in the autoregressive distributed-lag modeling framework," *Journal of Econometrics*, 188, 281–300.

DEB, P., D. FURCERI, D. JIMENEZ, S. KOTHARI, J. D. OSTRY, AND N. TAWK (2022a): "The effects of COVID-19 vaccines on economic activity," *Swiss Journal of Economics and Statistics*, 158, 1–25.

DEB, P., D. FURCERI, J. D. OSTRY, AND N. TAWK (2022b): "The economic effects of COVID-19 containment measures," *Open Economies Review*, 33, 1–32.

DI PORTO, E., P. NATICCHIONI, AND V. SCRUTINIO (2022): "Lockdown, essential sectors, and Covid-19: Lessons from Italy," *Journal of Health Economics*, 81, 102572.

FANG, H., L. WANG, AND Y. YANG (2020): "Human mobility restrictions and the spread of the novel coronavirus (2019-nCoV) in China," *Journal of Public Economics*, 191, 104272.

FORSYTHE, S., J. COHEN, P. NEUMANN, S. M. BERTOZZI, AND A. KINGHORN (2020): "The economic

and public health imperatives around making potential coronavirus disease–2019 treatments available and affordable," *Value in Health*, 23, 1427–1431.

GOEL, R. K., J. R. JONES, AND J. W. SAUNORIS (2023): "Explaining vaccine hesitancy: A COVID-19 study of the United States," *Managerial and Decision Economics*, 44, 1073–1087.

GUPTA, R. AND S. K. PAL (2020): "Trend analysis and forecasting of COVID-19 outbreak in India," *MedRxiv*, 2020–03.

HAMMOUDEH, S., W. MENSI, AND J. S. CHO (2022): "Spillovers between exchange rate pressure and CDS bid-ask spreads, reserve assets and oil prices using the quantile ARDL model," *International Economics*, 170, 66–78.

HANSEN, N.-J. H. AND R. C. MANO (2023): "COVID-19 vaccines: A shot in the arm for the economy," *IMF Economic Review*, 71, 148.

JERIS, S. S. AND R. D. NATH (2020): "Covid-19, oil price and UK economic policy uncertainty: evidence from the ARDL approach," *Quantitative Finance and Economics*, 4, 503–514.

JIANG, F., Z. ZHAO, AND X. SHAO (2022): "Modelling the COVID-19 infection trajectory: A piecewise linear quantile trend model," *Journal of the Royal Statistical Society Series B: Statistical Methodology*, 84, 1589–1607.

JIN, R. (2021): "The lag between daily reported Covid-19 cases and deaths and its relationship to age," *Journal of public health research*, 10, jphr–2021.

JING, X. AND J. S. CHO (2025): "Forecasting the confirmed COVID-19 cases using modal regression," *Journal of Forecasting*, 44, 1578–1601.

KIM, D. AND Y. J. LEE (2022): "Vaccination strategies and transmission of COVID-19: Evidence across advanced countries," *Journal of Health Economics*, 82, 102589.

KOUNTOURIS, Y. AND K. REMOUNDOU (2024): "Education and vaccine hesitancy: Evidence from the COVID-19 pandemic," *Economics Letters*, 240, 111768.

LEE, K. AND J. HWANG (2025): "Impact of underlying diseases and complications on COVID-19 mortality in South Korea: analysis of national health insurance service data," *Archives of Public Health*, 83, 20.

LIU, L., H. R. MOON, AND F. SCHORFHEIDE (2021): "Panel forecasts of country-level Covid-19 infections," *Journal of Econometrics*, 220, 2–22.

MCPHEDRAN, R. AND B. TOOMBS (2021): "Efficacy or delivery? An online discrete choice experiment to explore preferences for COVID-19 vaccines in the UK," *Economics Letters*, 200, 109747.

MEHTA, N., S. GUPTA, AND S. MAITRA (2023): "House prices and COVID-19 pandemic shocks in India: a nonlinear ARDL analysis," *International Journal of Housing Markets and Analysis*, 16, 513–534.

MORI, M., A. YOKOYAMA, A. SHICHIDA, K. SASUGA, T. MAEKAWA, AND T. MORIYAMA (2023): "Impact of sex and age on vaccine-related side effects and their progression after booster mRNA COVID-19 vaccine," *Scientific Reports*, 13, 19328.

OKADA, K. (2018): "Health and political regimes: Evidence from quantile regression," *Economic systems*, 42, 307–319.

OÂĂŹDRISCOLL, M., G. RIBEIRO DOS SANTOS, L. WANG, D. A. CUMMINGS, A. S. AZMAN, J. PAIREAU, A. FONTANET, S. CAUCHEMEZ, AND H. SALJE (2021): "Age-specific mortality and immunity patterns of SARS-CoV-2," *Nature*, 590, 140–145.

PADULA, W. V., S. MALAVIYA, N. M. REID, B. G. COHEN, F. CHINGCUANCO, J. BALLREICH, J. TIERCE, AND G. C. ALEXANDER (2021): "Economic value of vaccines to address the COVID-19 pandemic: A US cost-effectiveness and budget impact analysis," *Journal of Medical Economics*, 24, 1060–1069.

RAWLINGS, L., J. C. L. LOOI, AND S. J. ROBSON (2022): "Economic considerations in COVID-19 vaccine hesitancy and refusal: A survey of the literature," *Economic Record*, 98, 214–229.

RIBEIRO, T. F., G. M. CORDEIRO, F. A. PENA-RAMIREZ, AND R. R. GUERRA (2021): "A new quantile regression for the COVID-19 mortality rates in the United States," *Computational and Applied Mathematics*, 40, 255.

SILVA, F. R., M. SIMÕES, AND J. S. ANDRADE (2018): "Health investments and economic growth: a quantile regression approach," *International Journal of Development Issues*, 17, 220–245.

SUAH, J. L., M. HUSIN, P. S. K. TOK, B. H. TNG, T. THEVANANTHAN, E. V. LOW, M. R. APPANNAN, F. M. ZIN, S. M. ZIN, H. YAHAYA, ET AL. (2022): "Waning COVID-19 vaccine effectiveness

for BNT162b2 and CoronaVac in Malaysia: an observational study," *International Journal of Infectious Diseases*, 119, 69–76.

SUJATH, R. A. A., J. M. CHATTERJEE, AND A. E. HASSANIEN (2020): "A machine learning forecasting model for COVID-19 pandemic in India," *Stochastic Environmental Research and Risk Assessment*, 34, 959–972.

TAN, M., P. T. STRAUGHAN, AND G. CHEONG (2022): "Information trust and COVID-19 vaccine hesitancy amongst middle-aged and older adults in Singapore: A latent class analysis approach," *Social Science & Medicine*, 296, 114767.

TIU, A., Z. SUSSWEIN, A. MERRITT, AND S. BANSAL (2022): "Characterizing the spatiotemporal heterogeneity of the COVID-19 vaccination landscape," *American Journal of Epidemiology*, 191, 1792–1802.

TORRES, C., J. GARCÍA, F. MESLÉ, M. BARBIERI, F. BONNET, C. G. CAMARDA, E. CAMBOIS, A. CAPORALI, É. COUPPIÉ, S. PONIAKINA, ET AL. (2023): "Identifying age-and sex-specific COVID-19 mortality trends over time in six countries," *International Journal of Infectious Diseases*, 128, 32–40.

ULLAH, A., T. WANG, AND W. YAO (2022): "Nonlinear modal regression for dependent data with application for predicting COVID-19," *Journal of the Royal Statistical Society Series A: Statistics in Society*, 185, 1424–1453.

UTAMI, A. M., F. RENDRAYANI, Q. A. KHOIRY, D. NOVIYANTI, A. A. SUWANTIKA, M. J. POSTMA, AND N. ZAKIYAH (2023): "Economic evaluation of COVID-19 vaccination: A systematic review," *Journal of Global Health*, 13.

VERITY, R., L. C. OKELL, I. DORIGATTI, P. WINSKILL, C. WHITTAKER, N. IMAI, G. CUOMO-DANNENBURG, H. THOMPSON, P. G. WALKER, H. FU, ET AL. (2020): "Estimates of the severity of coronavirus disease 2019: a model-based analysis," *The Lancet infectious diseases*, 20, 669–677.

τ	$\zeta_*(\tau)$	$\beta_*(\tau)$	$\lambda_*(\tau)$	$\delta_*(\tau)$
0.1	-0.3323***	0.0120***	-2.2685***	0.0093***
	(0.0243)	(0.0012)	(0.1546)	(0.0013)
0.2	-0.2544***	0.0126***	-2.5575***	0.009***
	(0.0227)	(0.0009)	(0.2603)	(0.0012)
0.3	-0.2405***	0.0126***	-3.0958***	0.0082***
	(0.0231)	(0.0007)	(0.3469)	(0.0015)
0.4	-0.2129***	0.0129***	-3.1513***	0.0082***
	(0.0239)	(0.0009)	(0.3741)	(0.0013)
0.5	-0.1788***	0.016***	-3.3311***	0.0078***
	(0.0197)	(0.0012)	(0.3586)	(0.0014)
0.6	-0.1646***	0.0186***	-3.5187***	0.0088***
	(0.0294)	(0.0018)	(0.2636)	(0.0018)
0.7	-0.1315***	0.0238***	-3.7000***	0.0097***
	(0.0242)	(0.0028)	(0.2610)	(0.0018)
0.8	-0.0966**	0.0278***	-3.5458***	0.0093***
	(0.0297)	(0.0065)	(0.2190)	(0.0017)
0.9	-0.0760***	0.0391***	-3.6006***	0.0104***
	(0.0190)	(0.0100)	(0.1986)	(0.0012)
Wald Tests				
p-values	0.0004	0.0001	0.0795	0.6576

Table 1: QARDL ESTIMATION RESULTS. (i) QARDL estimation results are based on the following model: $\Delta D_t = \alpha_*(\tau) + \zeta_*(\tau) D_{t-1} + \gamma_*(\tau) C_{t-1} + \sum_{j=1}^{p-1} \lambda_{j*}(\tau) \Delta D_{t-j} + \sum_{j=0}^{q-1} \delta_{j*}(\tau) \Delta C_{t-j} + U_t(\tau) = \alpha_*(\tau) + \zeta_*(\tau)(D_{t-1} - \beta_*(\tau) C_{t-1}) + \sum_{j=1}^{p-1} \lambda_{j*}(\tau) \Delta D_{t-j} + \sum_{j=0}^{q-1} \delta_{j*}(\tau) \Delta C_{t-j} + U_t(\tau)$. (ii) Standard errors are in parentheses, and those for the long-run coefficient are calculated using the delta method. (iii) The p-values of the Wald tests are computed to test the hypotheses: $H_0^{\zeta} : \zeta_*(0.25) = \zeta_*(0.5) = \zeta_*(0.75), H_0^{\beta} : \beta_*(0.25) = \beta_*(0.5) = \beta_*(0.75), H_0^{\lambda} : \lambda_*(0.25) = \lambda_*(0.5) = \lambda_*(0.75), H_0^{\delta} : \delta_*(0.25) = \delta_*(0.5) = \delta_*(0.75)$. (iv) * indicates a significance level of $p < 0.05$, ** indicates a significance level of $p < 0.01$, and *** indicates a significance level of $p < 0.001$.

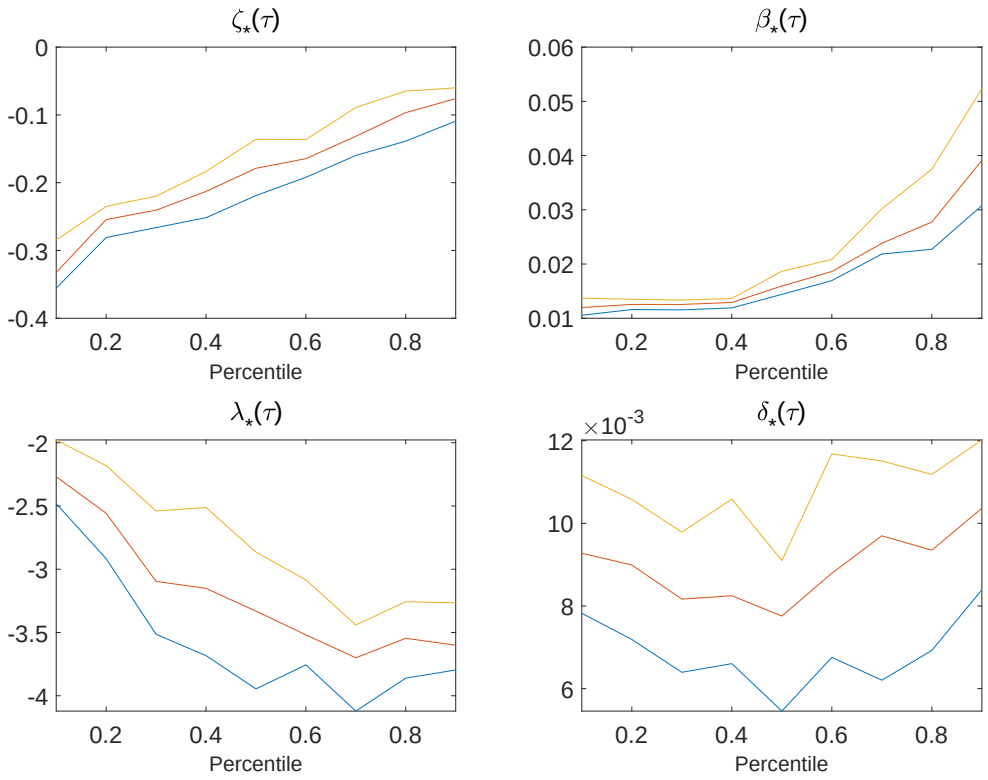

Figure 1: PARAMETER ESTIMATES USING THE WHOLE SAMPLE. The middle lines show the estimated parameters obtained by using all observations for different percentile levels: 0.1, 0.2, 0.3, 0.4, 0.5, 0.6, 0.7, 0.8, 0.9, along with 90% confidence bands.

Figure 2: PARAMETER ESTIMATES $\zeta_*(\tau)$, $\beta_*(\tau)$, $\lambda_*(\tau)$, AND $\delta_*(\tau)$ USING THE ROLLING WINDOW METHOD. The figures show the estimated parameters using the rolling window method with 90% confidence bands, and each window is constructed by 266 observations. Three different percentiles levels are employed: 0.25, 0.5, 0.75.

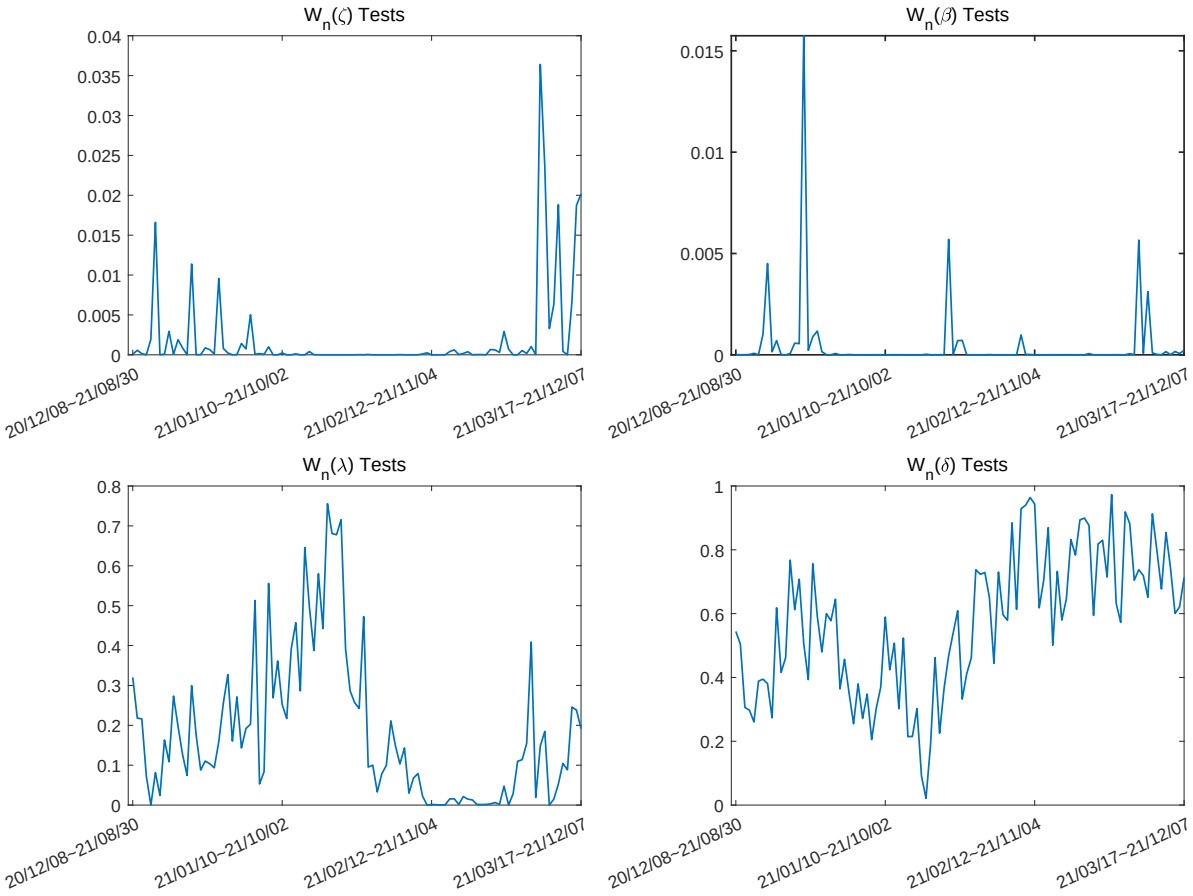

Figure 3: THE p-VALUES OF THE WALD TESTS. The figures show the estimated p-values of the Wald tests: (i) $\mathcal{W}_n(\beta)$ tests $H_0^\beta : \beta_*(0.25) = \beta_*(0.5) = \beta_*(0.75)$; (ii) $\mathcal{W}_n(\zeta)$ tests $H_0^\zeta : \zeta_*(0.25) = \zeta_*(0.5) = \zeta_*(0.75)$; (iii) $\mathcal{W}_n(\lambda)$ tests $H_0^\lambda : \lambda_*(0.25) = \lambda_*(0.5) = \lambda_*(0.75)$; and (iv) $\mathcal{W}_n(\delta)$ tests $H_0^\delta : \delta_*(0.25) = \delta_*(0.5) = \delta_*(0.75)$. The horizontal axis indicates the last observation of the window.